

Effects of O₂, H₂, and N₂ gases on the field emission properties of diamond-coated microtips

S. C. Lim, R. E. Stallcup II, I. A. Akwani, and J. M. Perez^{a)}
Department of Physics, University of North Texas, Denton, Texas 76203

(Received 6 May 1999; accepted for publication 28 June 1999)

We report the effects of O₂, H₂, and N₂ residual gases on the field emission properties of uncoated and diamond-coated individual Mo microtips. The microtips are made using electrochemical etching techniques and positioned 5 μm from the anode using a scanning tunneling microscopy system. We observe that the field emission (FE) current and turn-on voltage of diamond-coated microtips are significantly less degraded by O₂ exposure than those of uncoated Mo microtips. H₂ exposure enhances the FE properties of both uncoated and diamond-coated microtips, while N₂ exposure does not have any significant effect. © 1999 American Institute of Physics. [S0003-6951(99)02734-5]

Electron field emission (FE) from cold cathodes has recently attracted considerable interest due to potential applications in flat panel displays (FPDs) and vacuum electronics. In order to achieve FE from the surface of a material, a very high electric field must be used. To enhance the electric field near the surface, the material may be sharpened into a microtip. Materials that are used as microtips should be able to endure extremely high electrical stresses, achieve a high aspect ratio, and have good thermal conductivity. As a result, refractory metals such as Mo are currently used as microtips.^{1,2} However, metal microtips react with residual gases in vacuum containers such as O₂ resulting in an increase in the work function of the surface.³ In addition, the electric field near the microtip is high enough to ionize residual gases and the resultant ion bombardment of the microtip eventually results in failure of the microtip.⁴

Chemical vapor deposition (CVD) grown diamond has been reported to emit electrons at fields as low as 10 V/μm.⁵ A low field is advantageous in reducing ion formation and damage from ion bombardment. In addition, diamond is very inert and has a high thermal conductivity. Diamond coating of Si field emission arrays (FEAs)⁶ and individual Mo microtips,⁷ and diamond-like carbon coating of Mo FEAs⁸ have recently been reported to increase the FE current. The effects of Ne, He, H₂, and D₂ gases on the FE properties of diamond-coated Si microtips have been reported.⁹ In this letter, we report the effects of O₂, H₂, and N₂ on the FE properties of uncoated and diamond-coated individual Mo microtips.¹⁰ We observe that diamond-coated Mo microtips are significantly less affected by O₂ exposure than uncoated microtips.

The individual Mo microtips are made from Mo wire 0.020 in. in diameter using electrochemical etching techniques similar to those used in etching tips for scanning tunneling microscopy (STM). Typical etched Mo microtip apex diameters are ≤0.05 μm. To grow a diamond film on a Mo microtip, pre-seeding with 0.25 μm diamond powder is carried out using dielectrophoresis.⁷ To insure that only the smaller particles of the average 0.25 μm diamond powder

are in suspension, the solution is allowed to settle 1 h before dielectrophoresis. The seeded microtips are spot welded on a Mo wire and placed in a hot-tungsten filament CVD reactor. A thin diamond film is deposited for 60 min with a microtip temperature of 850 °C, and pressure of 30 Torr using H₂ and methane with flow rates of 200 and 1 sccm, respectively. The tungsten filament temperature is 2200 °C. Diborane at a concentration of 10 ppm relative to H₂ is introduced during growth to make the film conducting. The growth experiment is terminated by first shutting off the methane flow while maintaining the microtip, filament, and H₂ settings for 2 min. Then the filament, microtip heater, and H₂ flow are turned off in that order. Typical diamond-coated microtip apex diameters are ≤0.2 μm.

Materials under the influence of a strong electric field emit electrons that tunnel through a potential barrier according to the Fowler–Nordheim (FN) equation¹¹

$$I = AV^2 \exp\left(\frac{b\phi^{3/2}}{\beta V}\right),$$

where A and b are constants, ϕ is the work function, V the applied voltage, and β the geometric enhancement factor. The FE current is a sensitive function of the tip-anode distance. Therefore, it is important to precisely position the microtip with respect to the anode. We position the microtip using a STM system that uses a piezoelectric inchworm motor from Burleigh Instruments,¹² as shown in Fig. 1. The horizontal speed of the inchworm can be adjusted from approximately 4 to 0.5 mm/s. The horizontal speed is calibrated using an interferometer consisting of a He–Ne laser and a resonance cavity in which one of the mirrors is attached to the back of the inchworm, as shown in Fig. 1. The interferometer is used to calibrate the movement of the inchworm to an accuracy of ±0.02 μm. Using this system, different microtips can be positioned at the same distance from the anode with high accuracy.

The inchworm is housed in a vacuum system equipped with a quadrupole mass spectrometer at a base pressure ≤10⁻⁹ Torr. A microtip is loaded on the inchworm and the system is operated in STM mode. An atomically flat highly oriented pyrolytic graphite surface is used as the anode. The microtip approaches the anode until tunneling occurs at a

^{a)}Electronic mail: jperez@unt.edu

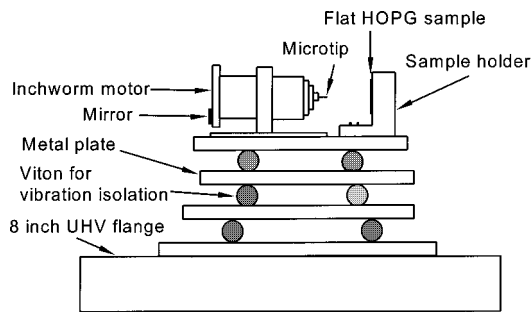


FIG. 1. Schematic of the microtip positioning system consisting of a piezoelectric inchworm motor operated as a scanning tunneling microscope to position the microtip 0.5–1.0 nm from the anode. The microtip is then retracted 5.00 ± 0.02 μm from the anode using an interferometer in which one of the mirrors is attached to the back of the inchworm. The viton spacers are used for vibration isolation.

tip-anode distance of 0.5–1.0 nm. The microtip is then retracted a distance of 5.00 ± 0.02 μm from the anode using the inchworm, and the STM feedback electronics are disengaged. Separate high-voltage electronics are used to measure the FE current versus voltage ($I-V$) curves. The microtip is cleaned of adsorbates in vacuum by biasing the microtip at a voltage of 500 V and FE current of 1×10^{-7} A for about 24 h until the variation in the FE current is less than 1%.

Before O_2 exposure, FE $I-V$ curves are measured at a pressure $\leq 10^{-9}$ Torr, as shown in Fig. 2 for 0 L exposure. In Fig. 2, the FE data are plotted $\ln(I/V^2)$ vs $1/V$ to allow comparison with the straight-line behavior predicted for FE by the FN equation. The inset in Fig. 2 shows the $I-V$ curves plotted using a log-linear scale. The small current on the order of 10^{-11} A observed below the threshold voltage for

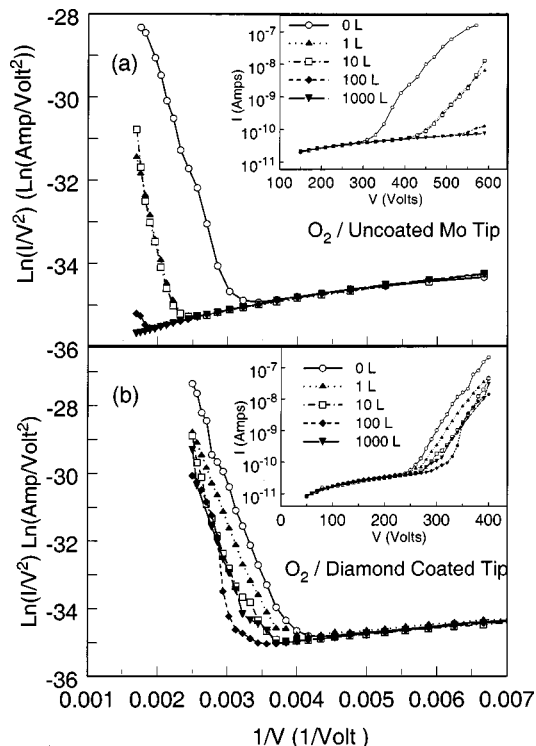


FIG. 2. (a) Fowler–Nordheim field emission current data for an uncoated Mo microtip after exposures to O_2 . (b) Fowler–Nordheim field emission current data for a diamond-coated Mo microtip after exposures to O_2 . The inset shows the corresponding field emission current vs voltage curves plotted using a log-linear scale.

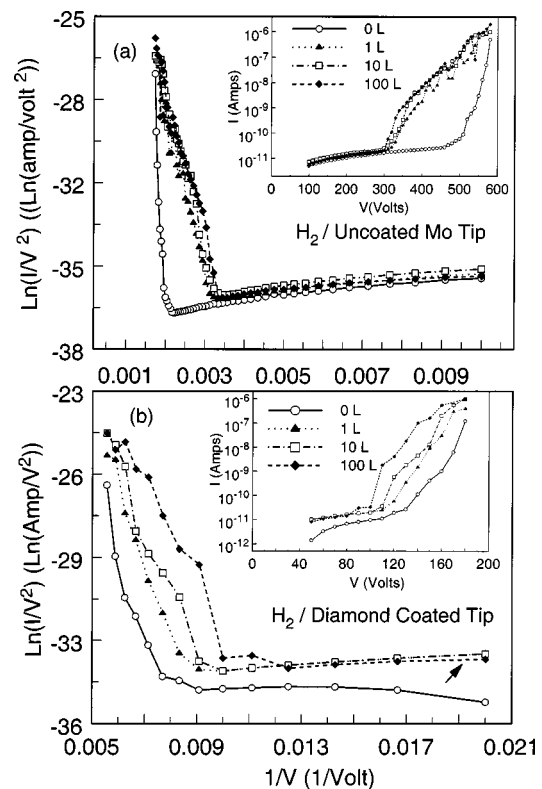


FIG. 3. (a) Fowler–Nordheim field emission current data for an uncoated Mo microtip after exposures to H_2 . (b) Fowler–Nordheim field emission current data for a diamond-coated Mo microtip after exposures to H_2 . The arrow indicates an increase in current below the threshold voltage for field emission. The inset shows the corresponding field emission current vs voltage curves plotted using a log-linear scale.

FE is due to leakage across the connectors. To achieve 1 L of exposure, O_2 is introduced into the vacuum system to a pressure of 2×10^{-7} Torr and the microtip is biased at a voltage that produces a FE current of 1×10^{-6} A for 5 s. After this exposure, the vacuum system is evacuated to $\leq 10^{-9}$ Torr and FE $I-V$ curves are measured, as shown in Fig. 2 for 1 L of exposure. In this manner, the microtip is not exposed to O_2 during the $I-V$ curve measurement. To achieve 10 L of exposure, O_2 is introduced again into the vacuum system to a pressure of 2×10^{-7} Torr and the microtip is biased at the same voltage for 50 s. Then, the system is evacuated to $\leq 10^{-9}$ Torr and the FE $I-V$ curves are measured, as shown in Fig. 2 for 10 L of exposure. This procedure is repeated for 100 and 1000 L of exposure.

As shown in Fig. 2(a), exposure of an uncoated Mo microtip to O_2 results in a decrease in the FE current, an effect that begins to appear after 1 L of exposure. Significant decrease in the FE current occurs after 100 L of exposure. After 1000 L of exposure, the FE current has completely disappeared. Before exposure, the FE current is approximately 2×10^{-7} A at 550 V. After 100 L of exposure, the FE current at this voltage decreases to approximately 7×10^{-11} A, a decrease of almost four orders of magnitude. As the O_2 exposure increases from 0 to 100 L, the turn-on voltage increases from approximately 300 to 525 V. Figure 2(b) shows the FE $I-V$ curves of a diamond-coated Mo microtip after exposures to O_2 . Exposure to 1 L of O_2 decreases the FE current at 400 V from 2×10^{-7} to 5×10^{-8} A, a decrease of about a factor of 4. Subsequent exposures decrease the FE current at

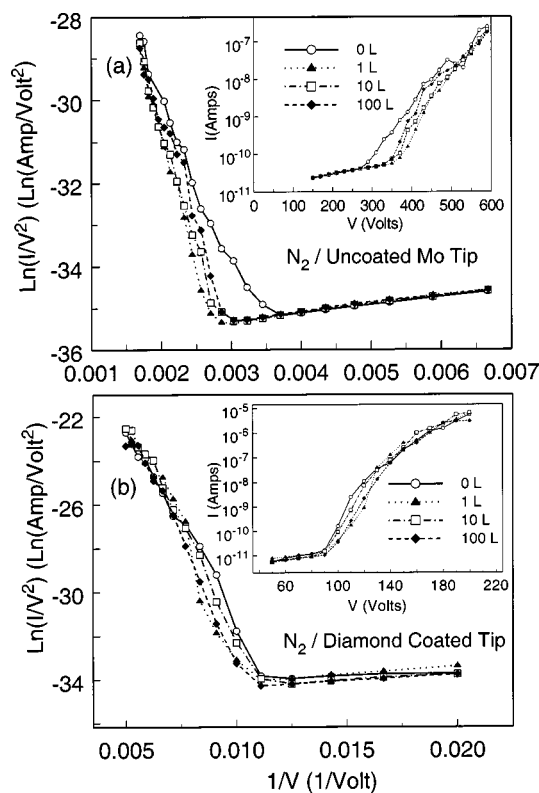


FIG. 4. (a) Fowler-Nordheim field emission current data for an uncoated Mo microtip after exposures to N_2 . (b) Fowler-Nordheim field emission current data for a diamond-coated Mo microtip after exposures to N_2 . The inset shows the corresponding current vs voltage curves plotted using a log-linear scale.

400 V to as low as 1×10^{-8} A. The turn-on voltage increases from about 250 to 300 V. By comparison, the FE current of an uncoated Mo microtip at 550 V decreases by almost four orders of magnitude after 100 L of exposure, and completely turns off after 1000 L of exposure.

As shown in Fig. 3(a), exposure of an uncoated Mo microtip to 1 L of H_2 results in an increase in FE current from 3×10^{-9} to 6×10^{-7} A at a tip bias of 550 V, and a significant reduction in turn-on voltage. This observation is consistent with reports of an increase in FE current from Mo FEAs after H_2 exposure.² After exposures of 10 and 100 L, the FE current at a bias of 550 V does not significantly change. As shown in Fig. 3(b), exposure of a diamond-coated Mo microtip to 1 L of H_2 results in an increase in the FE current and decrease in the turn-on voltage. After subsequent exposures, the FE current and turn-on voltage continue to increase and decrease, respectively. After 100 L of exposure,

the FE current at 160 V has increased from 3×10^{-9} to 1×10^{-6} A. After 1 L of exposure, an increase in current below the threshold voltage for FE is observed, indicated by the arrow in Fig. 3(b). This type of current observed below threshold after H_2 exposure has been previously reported and attributed to a hydrogen overlayer.⁶

As shown in Fig. 4(a), exposure of an uncoated Mo microtip to 1 L of N_2 results in an increase in the turn-on voltage and a slight decrease in the FE current. After subsequent exposures, very little change in the FE current near maximum current is observed. As shown in Fig. 4(b), exposure of a diamond-coated microtip to N_2 results in less change than that observed for an uncoated Mo microtip in Fig. 4(a). We conclude that at the exposures and tip-anode distances used, nitrogen ion sputtering does not significantly affect the FE properties of uncoated or diamond-coated Mo microtips.

In summary, we report that the FE properties of diamond-coated Mo microtips are significantly less degraded by O_2 exposure than those of uncoated Mo microtips. H_2 exposure significantly increases the FE current from uncoated and diamond-coated Mo microtips. N_2 exposure does not have a significant effect on the FE properties of uncoated or diamond-coated microtips, but degrades the properties of diamond-coated microtips less than those of uncoated microtips.

This work was supported, in part, by the Texas Advanced Research Program under award No. 003594053, and the National Science Foundation under award No. DMR-9311724.

¹C. A. Spindt, J. Appl. Phys. **39**, 3504 (1968).

²P. R. Schwoebel and I. Brodie, J. Vac. Sci. Technol. B **13**, 1391 (1995).

³R. Gomer, Surf. Sci. **38**, 373 (1973).

⁴I. Brodie and C. A. Spindt, Adv. Electron. Electron Phys. **83**, 1 (1992).

⁵M. W. Geis, N. N. Efremow, J. D. Woodhouse, M. D. McAleese, M. Marchywka, D. G. Socker, and J. F. Hochedez, IEEE Electron Device Lett. **27**, 1459 (1991).

⁶W. B. Choi, J. J. Cuomo, V. V. Zhirnov, A. F. Myers, and J. J. Hren, Appl. Phys. Lett. **68**, 720 (1996).

⁷F. Y. Chuang, C. Y. Sun, H. F. Cheng, C. M. Huang, and I. N. Lin, Appl. Phys. Lett. **68**, 1666 (1996).

⁸J. H. Jung, B. K. Ju, Y. H. Lee, J. Jang, and M. H. Oh, IEEE Electron Device Lett. **18**, 197 (1997).

⁹J. Liu, V. V. Zhirnov, W. B. Choi, G. J. Wojak, A. F. Myers, J. J. Cuomo, and J. J. Hren, Appl. Phys. Lett. **69**, 4038 (1996).

¹⁰S. C. Lim, Ph.D. dissertation, University of North Texas, 1998.

¹¹R. H. Fowler and L. Nordheim, Proc. R. Soc. London, Ser. A **119**, 683 (1928).

¹²Burleigh Instruments, Inc, Fishers, NY 14453.